^{13}C Kinetic Isotope Effects and the Mechanism of the Uncatalyzed Decarboxylation of Orotic Acid

Daniel A. Singleton,* Steven R. Merrigan, Bong J. Kim, Peter Beak,* Linda M. Phillips, and Jeehiun K. Lee*

Contribution from the Departments of Chemistry, Texas A&M University, College Station, Texas 77843, University of Illinois at Urbana Champaign, Urbana, Illinois 61801, and Rutgers, The State University of New Jersey, Piscataway, New Jersey 08854

Received September 20, 1999. Revised Manuscript Received February 16, 2000

Abstract: A complete set of ^{13}C kinetic isotope effects were determined for the thermal decarboxylation of 1,3-dimethylorotic acid and compared with theoretically predicted isotope effects for decarboxylation via either O-2 or O-4 protonated pathways. The best correspondence of experimental and calculated isotope effects is found for the O-4 protonated mechanism. This observation and the calculated reaction barriers support the previously predicted preference for this pathway. The preference for the O-4 protonated mechanism is found to result from a general predilection for O-4 protonation over O-2 protonation in the orotate/uracil series, and no significant extra stability appears associated with the formation of a formal carbene in the O-4 protonated decarboxylation. The carboxylate isotope effect for the uncatalyzed reaction is much smaller than the enzyme-catalyzed isotope effect recently reported, suggesting some divergence between uncatalyzed and enzyme-catalyzed mechanisms.

Introduction

The decarboxylation of orotidine 5′-monophosphate (OMP, **1**) to form uridine 5′-monophosphate (UMP, **2**) is an essential step in nucleic acid biosynthesis and is catalyzed by the enzyme orotidine 5′-monophosphate decarboxylase (ODCase).[1] ODCase is one of the most proficient enzymes known, with a $k_{cat}/K_m/k_{non}$ of 2.0×10^{23} M^{-1},[1] and this high proficiency makes the enzyme a target for the development of transition-state-analogue inhibitors with significant medical implications.[2] From a chemical perspective, the conversion of OMP to UMP is mechanistically unique; it is the only known biochemical decarboxylation in which the resultant carbanion intermediate does not have a π system into which to delocalize the negative charge.[3,4] The mechanism by which ODCase catalyzes OMP decarboxylation remains unknown.[1,5] After some debate, it is now believed that catalysis occurs without any aid from cofactors and metal ions.[6−11] Enzyme studies indicate a lysine that is important for catalysis, though not for binding.[12]

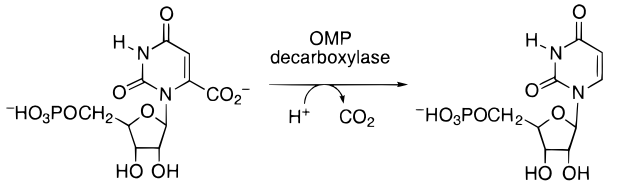

1 **2**

Despite the remarkable acceleration effected by the enzyme, the uncatalyzed decarboxylation has long been considered as a model for the catalyzed process. Beak and Siegel found that the rate of decarboxylation of 1,3-dimethylorotic acid in sulfolane at 206 °C could not be accounted for by reaction via the carboxylate anion **3a**,[5] and the authors concluded that this first-order reaction proceeds by decarboxylation of zwitterion **4a**. This zwitterion was also suggested to be important in the enzyme-catalyzed mechanism. Subsequent calculations by Lee and Houk support the idea of decarboxylation via a zwitterion-like species; the decarboxylation of O-2 protonated orotate **4b** is more favorable than the parent decarboxylation of orotate anion **3b** by 22 kcal mol^{-1}. However, the decarboxylation of *O-4 protonated orotate* **5b** is an even more favorable reaction by an additional 6 kcal/mol.[13] This facile decarboxylation for **5** was attributed to a contribution to the transition state that is illustrated by the stability of the product carbene **6**.

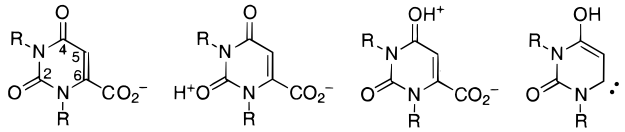

3 **4** **5** **6**

a R = CH_3 **b** R = H

* Address correspondence to this author at Texas A&M University.

(1) Radzicka, A.; Wolfenden, R. *Science* **1995**, *267*, 90−93.
(2) *Hereditary Orotic Aciduria and Other Disorders of Pyrimidine Metabolism*, 6th ed.; Suttle, D. P., Becroft, D. M. O., Webster, D. R., Eds.; McGraw-Hill: New York, 1989; Vol. I.
(3) Bruice, T. C.; Benkovic, S. *Bioorganic Mechanisms*; W. A. Benjamin: New York, 1966; Vol. 2.
(4) Bender, M. L. *Mechanisms of Homogeneous Catalysis from Protons to Proteins*; Wiley-Interscience: New York, 1971.
(5) Beak, P.; Siegel, B. *J. Am. Chem. Soc.* **1976**, *98*, 3601−3606.
(6) Acheson, S. A.; Bell, J. B.; Jones, M. E.; Wolfenden, R. *Biochemistry* **1990**, *29*, 3198−3202.
(7) Smiley, J. A.; Paneth, P.; O'Leary, M. H.; Bell, J. B.; Jones, M. E. *Biochemistry* **1991**, *30*, 6216−6223.
(8) Levine, H. L.; Brody, R. S.; Westheimer, F. H. *Biochemistry* **1980**, *19*, 4993−4999.
(9) Smiley, J. A.; Benkovic, S. J. *Proc. Natl. Acad. Sci. U.S.A.* **1994**, *91*, 8319−8323.
(10) Cui, W.; DeWitt, J. G.; Miller, S. M.; Wu, W. *Biochem. Biophys. Res. Commun.* **1999**, *259*, 133−135.
(11) Miller, B. G.; Traut, T. W.; Wolfenden, R. *J. Am. Chem. Soc.* **1998**, *120*, 2666−2667.
(12) Smiley, J. A.; Jones, M. E. *Biochemistry* **1992**, *31*, 12162−12168.

10.1021/ja993392m CCC: $19.00
Published on Web 03/25/2000

Scheme 1

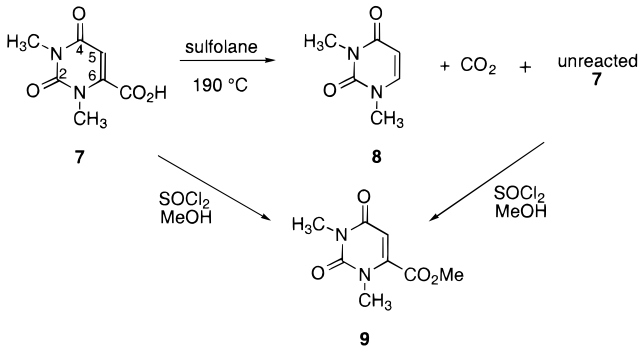

On the basis of the calculational prediction that the uncatalyzed decarboxylation proceeds via **5**, it was proposed that the ODCase-catalyzed decarboxylation of OMP proceeds through a similar intermediate. An energetic analysis indicated that this was a viable explanation for the remarkably proficient enzymatic catalysis.[13] It was also suggested at the time that decarboxylation occurred concerted with proton transfer to O-4, but Blanchard and co-workers have recently concluded that a stepwise mechanism must be in effect.[14]

We describe here a combined experimental and theoretical study of the uncatalyzed decarboxylation. A comparison of experimental and theoretically predicted kinetic isotope effects provides the first substantial experimental support for the O-4 protonation pathway for decarboxylation. At the same time, new calculations more closely resembling the uncatalyzed and biological systems provide a revised insight into the decarboxylation. The results substantiate the uncatalyzed mechanism and suggest some divergence of the uncatalyzed mechanism from the enzymatic mechanism.

Results and Discussion

Experimental Isotope Effects. The ^{13}C kinetic isotope effects (KIEs) for the decarboxylation of 1,3-dimethylorotic acid (**7**) were determined at natural abundance by recently reported methodology.[15] Samples of **7** on a 0.12−0.14 mol scale were decarboxylated in sulfolane at ∼190 °C in reactions taken to 92−95% completion, and unreacted **7** was recovered after conversion to the methyl ester (**9**) by chromatography (Scheme 1). The **9** obtained from the partial decarboxylation of **7** was analyzed by ^{13}C NMR along with standard samples of **9** formed from the same synthetic lot of **7**. The relative changes in ^{13}C composition for **9** were calculated using the N-3 methyl group as an "internal standard" with the assumption that its isotopic composition does not change.[16] From the changes in isotopic composition, the KIEs were calculated as previously described.[15] The resulting KIEs are summarized in Table 1.

The decarboxylation of **7** necessarily involves proton-transfer steps in addition to a decarboxylation step and an important question is whether the observed isotope effects reflect the intrinsic isotope effects for decarboxylation. Under these reaction conditions (except at 206 °C instead of 190 °C) Beak and Siegel found that the decarboxylation of **7** was first order to more that 90% conversion. If proton transfer by either another orotic acid molecule or an equilibrium-protonated solvent molecule were partially rate limiting, this would lead to a second-order component to the rate law. Direct intramolecular proton transfer from the carboxyl to O-4 or O-2 would not appear feasible. The C6 isotope effect of 1.025−1.030 is substantial for 190 °C, and may be compared to that observed for the α carbon in decarboxylations of oxalic acid (1.025−1.032 at 98−135 °C).[17] From this observation, the first-order kinetics, and the general expectation that the exothermic proton transfers reverting **4a** or **5a** back to starting material will be faster than decarboxylation (predicted below to have a barrier of ∼8 kcal/mol), we conclude that decarboxylation is essentially fully rate limiting.

Table 1. Experimental and Calculated ^{13}C KIEs ($k^{12}C/k^{13}C$) for Decarboxylation at 190 °C

Experimental KIEs (**7**)					
exp	C2	C4	C5	C6	CO_2
1	1.002(3)	1.002(4)	1.002(4)	1.025(6)	1.013(5)
2	1.001(3)	0.998(3)	1.004(3)	1.027(3)	1.013(2)
3	1.002(3)	1.000(3)	1.005(2)	1.030(2)	1.013(3)
4	0.998(3)	1.001(4)	1.003(4)	1.029(4)	1.010(3)
Calculated KIEs (**11**)					
r,[a] Å	C2	C4	C5	C6	CO_2
(a) via **13** → **15** → **17**					
2.2	1.002	1.001	1.005	1.026	1.028
2.4	1.002	1.001	1.003	1.025	1.024
2.65	1.002	1.000	1.004	1.028	1.015
(b) via **12** → **14** → **16**					
2.2	0.999	1.006	1.003	1.025	1.029
2.4	0.999	1.007	1.004	1.028	1.024
2.7	0.999	1.008	1.005	1.031	1.014

[a] The distance *r* is between the carboxylate carbon and the orotate C_6.

Theoretical Decarboxylation Pathways. Reflection on the use of energies of decarboxylation of **4b** and **5b** as models for either the enzymatic decarboxylation of **1** or the thermal decarboxylation of **7** suggested two concerns. The first concern is the use of reaction energies instead of activation barriers. The latter should obviously be more accurate, and the calculation of transition structures is necessary for the prediction of kinetic isotope effects for comparison with the experimental values. A complication is that the potential energy surface around the transition state for decarboxylation of **3**−**5** is almost flat (the reverse reactions are nearly enthalpically barrierless), and the geometry of a calculated potential energy saddle point may differ from the actual transition state geometry due to a number of factors. A second concern is whether error is introduced by using a hydrogen on N-1 as in **4b** and **5b** instead of the methyl group of **7** or the ribose residue of **1**. An alkyl group on N-1 might sterically accelerate the decarboxylation and would likely counter the planar symmetry found in calculated structures for **4b** and **5b**. In addition, a hydrogen bond between the N-1 hydrogen and the carboxylate in **4b** or **5b**, as depicted in **10**, could artificially stabilize these structures, particularly for **4b**,

(13) Lee, J. K.; Houk, K. N. *Science* **1997**, *276*, 942−945.
(14) Ehrlich, J. I.; Hwang, C.-C.; Cook, P. F.; Blanchard, J. S. *J. Am. Chem. Soc.* **1999**, *121*, 6696.
(15) Singleton, D. A.; Thomas, A. A. *J. Am. Chem. Soc*. **1995**, *117*, 9357−9358.
(16) The relative ^{13}C isotopic compositions for each of the three methyl groups of **9** is unchanged, within experimental error, between samples of **9** recovered from partial conversion of **7** versus standard samples of **9**. This supports the postulate that the N-3 methyl group's isotopic composition is unchanged. The choice of N-1 versus N-3 methyl carbons as internal standard has no effect on the isotope effects obtained, within experimental error.
(17) Buddenbaum, W. E.; Hallem, M. A.; Yankwich, P. E. *J. Chem. Phys.* **1967**, *71*, 2929.

Scheme 2

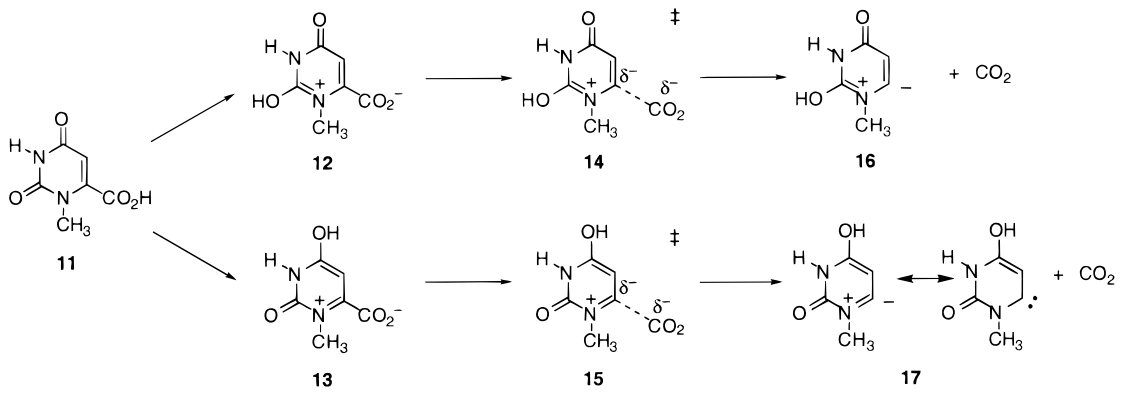

and distort the energetics of their reactions. This is found to be the case (vide infra). Consequently, 1-methylorotic acid (**11**) was used as the calculational model.

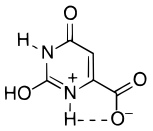

10

The pathways for decarboxylation of **11** via the 2-protonated zwitterion **12** and the 4-protonated zwitterion **13** were explored in Becke3LYP calculations using a 6-31+G* basis set (Scheme 2).[18] Decarboxylation of **12** affords the zwitterion **16**, while decarboxylation of **13** affords **17**, describable as a resonance hybrid of a zwitterion and a carbene. To explore the free-energy surface in the area of the transition states for decarboxylation, the distance *r* between the carboxylate carbon and C_6 was varied iteratively, fully optimizing all other coordinates. At each point the free energy was estimated as $\Delta E - T\Delta S$ by including zero-point energies and entropies based on the unscaled vibrational frequencies.[19] Very broad fully optimized potential energy saddle points were located with $r = 2.41$ Å for the decarboxylation of **12** and $r = 2.38$ Å for the decarboxylation of **13**. A measure of the flatness of the surface around the potential energy saddle points is that the energy (including ZPE) is predicted to vary by only ~0.7 kcal/mol as the distance *r* is varied from 2.15 to 2.8 Å.

The potential energy and free-energy profiles for these decarboxylations are shown in Figure 1. Because the neutral **7** is the species actually present in the experimental system,[5] the neutral calculational model **11** is the appropriate reference state for calculation of the overall reaction barriers. Entropy increases uniformly as *r* is increased, and allowing for entropy has the effect of shifting the free-energy maximum to earlier than the potential energy saddle point. For both pathways the free-energy maximum is predicted to occur at $r \approx 2.2$ Å. A shallow potential energy minimum was found for each at $r \approx 2.91$ Å; this minimum disappears when entropy is taken into account. For the lower energy pathway involving the 4-protonated **13**, the

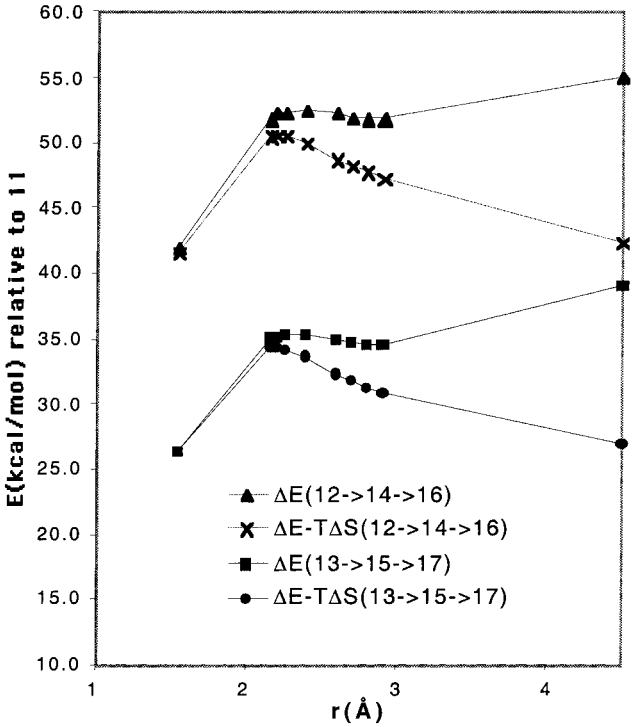

Figure 1. Potential energy (ΔE including zero-point energy) and free energy (approximated as $\Delta E - T\Delta S$) profiles for the decarboxylation of **12** and **13**, relative to the starting material **11**.

predicted free-energy barrier for decarboxylation at 190 °C is 34.3 kcal/mol. The predicted rate at 206 °C is 2×10^{-3} s^{-1}, in very reasonable agreement with the previously observed rate for decarboxylation of **7** of 7.6×10^{-4} s^{-1}.[5] The barrier for decarboxylation via the 2-protonated **12** is substantially higher at 50.5 kcal/mol.

The previously observed 6 kcal/mol preference for the decarboxylation of **5b** over the decarboxylation of **4b** is not observed with **13** versus **12**. A point of confusion arises when comparing the results here to those of Lee and Houk, because their work compared barriers starting from the differing zwitterions instead of a single reference state. If that were done in the present work, protonation of either carbonyl would catalyze the decarboxylation about equally, as the barriers for decarboxylation of **12** and **13** are 8.4 and 7.6 kcal/mol, respectively. The higher barrier predicted for decarboxylation of **4b** appears largely to be an artifact of the presence in this simplified model of the hydrogen bond shown in **10**, artificially stabilizing the starting material and making the barrier for decarboxylation of the O-2 protonated **4b** look high.

(18) Recent results suggest that the Becke3LYP method underestimates somewhat the barrier for decarboxylation but provides reliable relative energetics. See: Bach, R. D.; Canepa, C.; Glukhovtsev, M. N. *J. Am. Chem. Soc.* **1999**, *121*, 6542. Bach, R. D.; Canepa, C. *J. Am. Chem. Soc.* **1997**, *119*, 11725. Becke3LYP/6-31+G* calculations were previously found to give a reasonably accurate prediction of the barrier for the orotate decarboxylation (see ref 13).

(19) For calculating the entropy the frequency of the normal mode associated with the reaction coordinate was omitted, even when this frequency was real.

To properly compare the O-2 and O-4 protonated pathways a common energetic standard is required. For the uncatalyzed reaction the starting material **11** is isomeric with the two pathways, allowing the direct calculation of the reaction barrier. This leads to a revised understanding of the proton catalysis of decarboxylation. Figure 1 makes it clear that decarboxylation via the 4-protonated pathway would still be strongly preferred over the 2-protonated pathway. However, this preference is best understood as resulting from a general predilection for O-4 protonation over O-2 protonation in the orotate/uracil series. Both **13** and **17** are more stable than their O-2 protonated counterparts, **13** by 15.7 kcal/mol over **12** and **17** by 15.9 kcal/mol over **16**. The greater stability of the O-4 protonated pathway remains essentially constant between starting materials, transition structures, and products.

There is thus no significant extra stability associated with the carbene **17**. If, as previously proposed, decreased charge separation is a factor in the greater stability of **17** over **16**, this must be a nearly equal factor in the greater stability of **13** over **12**. However, O-4 protonation remains strongly favored with the neutral 1-methyluracil − **18** is predicted to be more stable than **19** by 12.0 kcal/mol (Becke3LYP/6-31+G* + zpe) − so decreased charge separation in the carbene **17** or zwitterion **13** appears at best a minor factor in the preference for O-4 protonation.

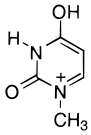

18

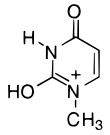

19

Predicted vs Experimental Isotope Effects. Isotope effects for the decarboxylation of **12** and **13** were calculated[20] at several values of *r*. Table 1 shows the predicted KIEs for each at 2.2 Å, corresponding to the approximate predicted free-energy maximum, at 2.4 Å, corresponding approximately to the potential energy maximums, and at 2.65 or 2.7 Å, chosen to give a best fit with the experimental KIEs. The isotope effect for C6 and the carboxylate carbon change significantly with changing *r*, precluding their use in assigning the mechanism to the O-2 protonated versus O-4 protonated pathways, but the isotope effects for C2, C4, and C5 vary little with *r*. Of these, only C4 shows substantially different predicted isotope effects. When O-2 is protonated, the C−N and C−C bonds to C4 lose some partial double bond character and become weaker. As a result, a significant secondary carbon isotope effect (1.006−1.008) is predicted for C4 in the decarboxylation of **12**. No net decrease in bonding to C4 occurs on the O-4 protonated pathway and the predicted isotope effect is near unity. In the event, the experimental results at C4 are all within error of the prediction for the decarboxylation of **13**. This provides significant experimental support for the theoretically predicted preference for decarboxylation of the O-4 protonated intermediate.[21]

The predicted KIE for the carboxylate carbon varies substantially with *r*. As *r* increases, the predicted KIE decreases, and at the extreme of complete decarboxylation to CO_2 the predicted equilibrium KIE is 0.992. The best overall fit of the experimental KIEs with those predicted for the O-4 protonated pathway occurs with $r = 2.65$ Å. This suggests that the transition state for the actual decarboxylation in solution is later than either the estimated free-energy maximum or the potential energy maximum. Why should this be? One possible explanation is that the catalytic effectiveness of the carbonyl protonation is mitigated in solution by hydrogen bonding to the sulfolane solvent. In the extreme of the decarboxylation of the anion **20**, the predicted free-energy maximum occurs at $r = 3.55$ Å, and no potential energy maximum short of complete decarboxylation can be found. The effective partial removal of the catalytic proton by hydrogen bonding to solvent would therefore be expected to shift the transition state later. To test this idea, the pathway for decarboxylation of **13** was recalculated with the addition of a water molecule hydrogen bonded to the O-4 proton, as in structure **21**. As a result, the potential-energy maximum

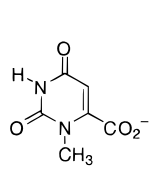

20

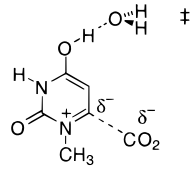

21

shifts from 2.38 Å to 2.54 Å. An additional factor that may shift the transition state for decarboxylation later in solution relative to that predicted in the gas phase is the stabilizing effect of the polar solvent ($\epsilon = 42.13$) on the charge separation in the zwitterion **13**. This charge separation decreases as the decarboxylation proceeds toward **17**, and the decreasing stabilization by the polar solvent will tend to shift the transition state later. Overall, the hypothesis that the actual transition state is later than calculationally predicted appears reasonable, and the later transition state provides the best correlation of the experimental and theoretical isotope effects.

Comparison with the Enzymatic Mechanism. Blanchard and co-workers have recently reported a carboxylate ^{13}C isotope effect of 1.043 ± 0.003 for the *E. coli* ODCase-catalyzed decarboxylation of OMP.[14] This is very different from the ∼1.013 observed here for the uncatalyzed reaction, and suggests a substantially earlier transition state (in terms of CO_2 loss) than in the uncatalyzed process. In an additional observation, the enzyme-catalyzed carboxylate isotope effect decreased to 1.034 ± 0.002 in D_2O, indicative of a mechanism in which two steps are competitively rate limiting. This would be surprising for a mechanism analogous to the uncatalyzed process. The predicted barrier for decarboxylation of an intermediate O-4 protonated zwitterion is still substantial (∼8 kcal/mol for **13**), and it would be unusual for a proton-transfer or binding step to have an equally energetic barrier height relative to the zwitterion. Both of these observations would tend to weigh against a close analogy between uncatalyzed and enzyme-catalyzed mechanisms. Perhaps this is to be expected, considering the substantial difference in the reaction conditions.

(20) (a) Bigeleisen, J.; Mayer, M. G. *J. Chem. Phys.* **1947**, *15*, 261. (b) Wolfsberg, M. *Acc. Chem. Res.* **1972**, *5*, 225. (c) The calculations used the program QUIVER (Saunders, M.; Laidig, K. E.; Wolfsberg, M. *J. Am. Chem. Soc.* **1989**, *111*, 8989) with Becke3LYP frequencies scaled by 0.9614. (Scott, A. P.; Radom, L. *J. Phys. Chem.* **1996**, *100*, 16502.). Tunneling corrections (Bell, R. P. *The Tunnel Effect in Chemistry*; Chapman & Hall: London, 1980; pp 60−63) were negligible.

(21) An alternative possibility suggested by a referee is decarboxylation of the carboxylate anion (**3**, R = CH_3). The predicted isotope effects for this decarboxylation are 1.001, 1.005, 1.007, 1.030, and 1.008 at C2, C4, C5, C6, and the carboxylate, respectively, which does not fit as well with the experimental values. Beak and Siegel (see ref 5) had previously ruled out decarboxylation of the carboxylate anion based on kinetic considerations.

Conclusion

The combination of new theoretical calculations and isotope effects supports the previously predicted O-4 protonation pathway for the uncatalyzed decarboxylation. However, some of the previous ideas regarding this decarboxylation and their implications toward the enzyme-catalyzed process are not supported. Protonation of either O-2 or O-4 of orotates catalyzed the decarboxylation, but the barrier for decarboxylation after protonation for 1-alkylorotates is essentially equivalent along the two pathways. The previous suggestion that the remarkable proficiency of ODCase is due to the stability of a carbene intermediate is not supported. The O-4 protonated pathway is still strongly favored for the uncatalyzed reaction, but this is best ascribed to a general preference for O-4 protonation in orotates and uracils. Of course, the enzyme may catalyze the decarboxylation via the disfavored but nevertheless highly catalyzing O-2 protonation or by some divergent mechanism.

Experimental Section

Decarboxylation of 1,3-Dimethylorotic Acid: Example Procedure. A mixture of 22.1 g (0.12 mol) of 1,3-dimethylorotic acid (**7**) and 360 mL of sulfolane was heated to 190 °C while a stream of nitrogen was passed over the reaction mixture and bubbled through four saturated barium hydroxide solutions in series. The percent conversion of the reaction after 2 h based on precipitated barium carbonate was 92%. The sulfolane solvent was removed by vacuum distillation and the residue was then dissolved in 25 mL of anhydrous methanol and 16 mL of thionyl chloride was slowly added in an ice bath. The resulting solution was stirred for 1 h at 25 °C and then refluxed for 17 h. Flash chromatograph on silica gel using 9:1 CH_2Cl_2/ethyl acetate as eluent followed by recrystallization from hexane/ethyl acetate afforded 1.2 g (5%) of the methyl ester **9**. A standard sample of **9** was prepared from the starting **7** in an identical fashion.

NMR Measurements. Mixtures of 100 mg of **9** in $CDCl_3$ at a height of 5.0 cm in a 5 mm NMR tube were used for all ^{13}C NMR measurements, and all measurements were taken at a fixed temperature of 40 °C. A T_1 determination by the inversion−recovery method was carried out for each NMR sample, and the T_1's were found to remain constant from sample to sample.

The ^{13}C spectra were obtained locked on $CDCl_3$ at 125 MHz on a Varian XL500 broadband NMR spectrometer, using inverse gated decoupling, calibrated $2\pi/9$ pulses, and 120 s delays between pulses. To obtain sufficient digital resolution (5 points/$\nu_{1/2}$ is minimal), a 158720 point FID was zero-filled to 256K points before Fourier transformation. Integrations were determined numerically using a constant integral region set at 5 times the typical peak width at 1/2 height for each peak. A zeroth-order baseline correction was generally applied, but in no case was a first-order (tilt) correction applied.

Table 2. Average ^{13}C Integrations

% completion	C2	C4	C5	C6	CO_2	*n*
91%	1115(6)	1114(9)	1154(7)	1195(6)	1139(6)	10
standard	1109(7)	1109(6)	1148(8)	1126(6)	1103(7)	10
R/R_0	1.005	1.004	1.006	1.062	1.033	
92%	1099(4)	1076(7)	1130(3)	1182(7)	1127(5)	10
standard	1096(8)	1080(5)	1118(8)	1106(3)	1092(5)	10
R/R_0	1.002	0.996	1.011	1.068	1.032	
92.5%	1159(7)	1136(6)	1191(6)	1254(6)	1174(7)	9
standard	1153(5)	1135(5)	1175(4)	1162(2)	1137(7)	9
R/R_0	1.006	1.001	1.013	1.079	1.033	
95%	1091(8)	1082(9)	1129(11)	1204(11)	1123(8)	10
standard	1097(6)	1078(8)	1120(10)	1106(6)	1090(6)	10
R/R_0	0.994	1.003	1.008	1.088	1.031	

Results from All Reactions. ^{13}C measurements were carried out for a total of 4 reactions. The integration of the N-3 methyl carbon in each spectrum was set at 1000. The average integrations for the other carbons for each reaction, along with the standard results for the starting materials, are shown in Table 2 along with the standard deviation of the observed values in parentheses. In each case *n* is the total number of spectra obtained. The values for R/R_0 were calculated as the ratio of average integrations relative to the standard. The isotope effects and errors were then calculated as previously described.[15] The error calculations used the standard deviations in R/R_0 ($\Delta R/R_0$, calculated from eq 1 where ΔIntSample and ΔIntStandard are standard deviations in the integrations for the sample and standard, respectively) and assumed errors of ±4% for the first reaction and ±0.5% for the latter three reactions. (The uncertainty in the first reaction's conversion was high because it was based on the amount of recovered **9**.)

$$\Delta R/R_0 = (R/R_0)((\Delta\text{IntSample}/\text{IntSample})^2 + (\Delta\text{IntStandard}/\text{IntStandard})^2)^{1/2} \quad (1)$$

Acknowledgment. We thank the NIH (Grant Nos. GM-45617 and GM-18874), the ACS-PRF (Grant No. 32732-G4), the Busch Grant Program, and The Robert A. Welch Foundation for support and NSF grant Nos. CHE-9528196 and CHE-9526355, the Texas A&M University Supercomputing Facility and the National Center for Supercomputing Applications, and the Boston University Scientific Computing Facilities for computational resources. B.J.K. thanks KRICT for support. We also thank Steven Ealick for a preliminary description of a crystal structure of ODCase.

Supporting Information Available: Energies and full geometries of all calculated structures (PDF). This material is available free of charge via the Internet at http://pubs.acs.org.

JA993392M